

Modelling of molecular bonding with a cohesive zone model strategy

R. Estevez^{1,*}, G Parry¹, P. Mc Garry²

¹ Université de Grenoble, SIMaP, UMR CNRS 5266, Grenoble-INP, UJF, 1130 rue de la piscine, BP75, F-38402 St Martin d'Hères cedex, France

² College of Engineering and Informatics, Mechanical and Biomedical Engineering
National University of Ireland, Galway, University Road, Galway, Ireland

* Corresponding author: Rafael.Estevez@simap.grenoble-inp.fr

Abstract Molecular or direct bonding is an emerging technique to assemble directly two silicon wafers or metal parts. In vacuum, the two surfaces are free to bond perfectly if their lattice orientation is coincident. When defects have to be considered like a misorientation or when bonding is processed in air, a slowdown of the bonding velocity is observed and its efficiency in term of adhesion energy decreased. The aim of this project is to gain insight in the bonding process and to investigate the influence of the bonding characteristics. A specific strategy based on a non linear contact mechanics scheme is adopted to describe the bonding process: the methodology is shown to provide enough flexibility to account for the normal and tangential interactions. These latter are described with Traction-Opening displacement laws that are first derived from interatomic potential. the influence on the bonding characteristic on the bonding wavefront is investigated to attempt deriving local information of the bonding mechanism.

Keywords Cohesive model, molecular bonding, finite element simulation

1. Introduction

Molecular bonding is nowadays used in the microelectronics industry to assemble directly parts with no use of a gluing layer. The technique is based on the natural adhesion between clean surfaces that come close to each other. The technique is shown efficient when performed in vacuum (see for instance the review by Prössl and Kräuter [1] and references therein). One of the challenges for improving this technique is to perform the bonding in air instead of vacuum which induces problems related to the air wedge generated in the vicinity of the process zone (see for instance Rieutord et al. [2]). Among the features that need to be handled carefully is the estimation of the adhesion energy and the stress induced by the processing in the wafer. Wedge tests are performed to measure the interface energy with the so called Maszara configuration (see [3] for a review). An alternative to the Maszara test, which is not so easy to handle, is to adopt an inverse approach based on the observation of the bonding wavefront during the adhesion process. The present study focuses on this aspect. The goal is to identify the adhesion energy from the observation of the bonding wavefront profile and its velocity. To this end, a modelling of the molecular bonding is presented here that is based on a cohesive description of the molecular interactions between two Silicon wafers. The work is restricted to bonding in vacuum. The cohesive description is first postulated but could be atomistically informed with molecular dynamics simulations as reported by Kubair et al. [4] for instance.

We first describe the modelling strategy and next, present a typical simulation of molecular bonding performed with the finite element package abaqus [5]. The approach is shown able to capture qualitatively observations reported in the literature. This work precedes a parametric study currently under progress.

2. Modelling and simulation the continuum scale

2.1 Problem formulation

The two wafers are modeled as circular plates, of diameter 200 mm and thickness 0.7 nm. A linear elastic constitutive law is chosen, with values of Young's modulus $E=100$ GPa and Poisson's ration $\nu = 0.22$, typical from Si. The geometry and boundary conditions of the system are depicted in Fig.1, where only the top wafer is represented. A symmetry boundary condition is imposed along a diameter. The two wafers are originally distant from a few nanometers. A pressure is applied over an area along the edge of the upper wafer. By pushing the two wafers together, they are coming in sufficiently close contact to activate the attraction between the two surfaces. A bonding wave is hence triggered from this area, spreading all along the interface between the wafers.

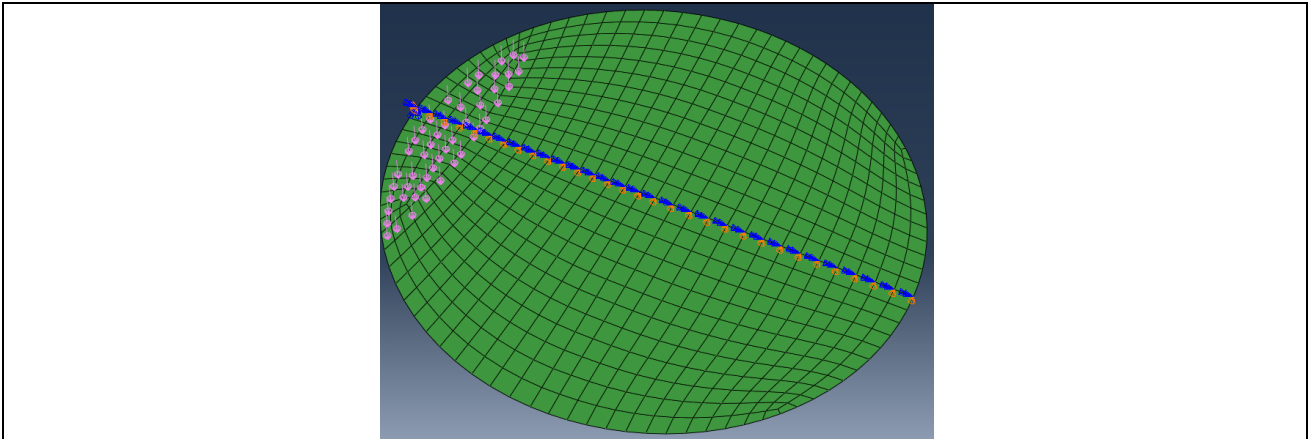


Figure 1: schematic description of the boundary conditions prescribed on the top wafer. Symmetry boundary conditions are enforced along one diameter. A pressure is applied on a small area along one edge in order to trigger the bonding process.

It is critical to model properly the interaction between the two surfaces. The Xu and Needleman (XN) cohesive model [6] is used to describe the interface behaviour. This formulation show a Traction-Separation similar to that reported in Kubair et al. [4] and therefore adopted for the case reported here. It is based on the definition of an interface potential, \emptyset , representing the work done when two opposing surfaces at an interface undergo a relative separation $\underline{\Delta}$. The resulting tractions are given by;

$$\underline{T}(\underline{\Delta}) = \partial\emptyset(\underline{\Delta})/\partial\underline{\Delta} \quad (1)$$

The interface potential is given by;

$$\emptyset(\Delta_n, \Delta_t) = \emptyset_n + \emptyset_n \exp\left(-\frac{\Delta_n}{\delta_n}\right) \left[\left\{ 1 - r + \frac{\Delta_n}{\delta_n} \right\} \left(\frac{1-q}{r-1} \right) - \left\{ q + \left(\frac{r-q}{r-1} \right) \frac{\Delta_n}{\delta_n} \right\} \exp\left(-\frac{\Delta_t^2}{\delta_t^2}\right) \right] \quad (2)$$

Coupling in this model is controlled through the parameters q and r ;

$$\text{where, } q = \phi_t / \phi_n \quad r = \Delta_n^* / \delta_n$$

ϕ_n and ϕ_t are the work of normal and tangential separation respectively. The normal and tangential components of the interface separation vector, $\underline{\Delta}$, are Δ_n and Δ_t respectively. The normal and tangential interface characteristic lengths are δ_n and δ_t respectively and Δ_n^* is the value of Δ_n after complete tangential separation takes place under the condition of normal tension being zero ($T_n = 0$).

Using equations (1) and (2), the interfacial tractions are obtained as follows;

$$T_n = \frac{\partial \phi}{\partial \Delta_n} = \left(\frac{\phi_n}{\delta_n} \right) \exp \left(-\frac{\Delta_n}{\delta_n} \right) \left\{ \frac{\Delta_n}{\delta_n} \exp \left(-\frac{\Delta_t^2}{\delta_t^2} \right) + \frac{1-q}{r-1} \left[1 - \exp \left(-\frac{\Delta_t^2}{\delta_t^2} \right) \right] \left[r - \frac{\Delta_n}{\delta_n} \right] \right\} \quad (3)$$

$$T_t = \frac{\partial \phi}{\partial \Delta_t} = 2 \left(\frac{\phi_n}{\delta_n} \right) \left(\frac{\delta_n}{\delta_t} \right) \frac{\Delta_t}{\delta_t} \left\{ q + \left(\frac{r-q}{r-1} \right) \frac{\Delta_n}{\delta_n} \right\} \exp \left(-\frac{\Delta_n}{\delta_n} \right) \exp \left(-\frac{\Delta_t^2}{\delta_t^2} \right) \quad (4)$$

The characteristic lengths δ_n and δ_t are given by;

$$\delta_n = \phi_n / (Tn_{max} \exp(1)) \quad (5)$$

$$\delta_t = \phi_t / (Tt_{max} (0.5 \exp(1))^{0.5}) \quad (6)$$

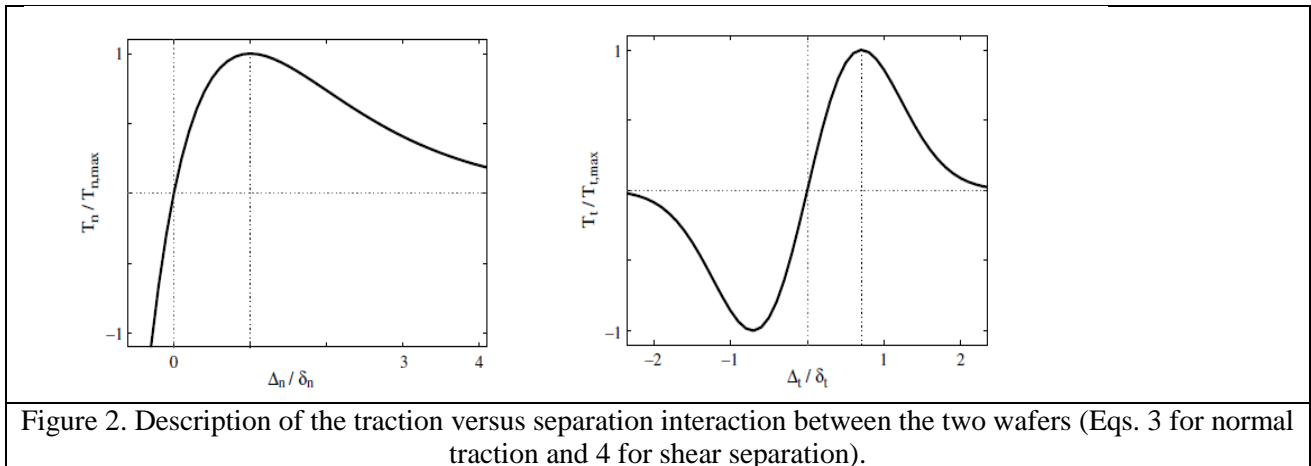
Where Tn_{max} is the maximum normal traction without tangential separation and Tt_{max} is the maximum tangential traction without normal separation. Typical shapes of the tractions are depicted in Fig. 2. It is worth noting that this constitutive law managing the interactions between the two surfaces is strongly nonlinear.

Practically, we have used $q=1$ and $r=0$, a maximum traction of 1GPa and characteristic opening $\delta_n=\delta_t=1\text{nm}$. The traction-opening profiles are reported in Fig. 2.

A viscosity term has been added according to [7] in order to avoid instability problems during the decay in the traction with opening (see Fig. 2), in the event of a strong drop in stiffness during loading (e.g. a snap-through).

The calculation are carried out using the finite element code ABAQUS [5]. The interaction between the two surfaces is accounted for through a non linear contact mechanics algorithm. The tractions representing the bonding are taken from (3-4) and implemented in Abaqus in a User INTERface routine (UINTER). The non linear contact scheme is implemented using a user subroutine linked to the implicit FEM solver. The methodology is shown to provide enough flexibility to account for the

normal and tangential interactions. Unlike the cohesive elements methods, it is easy to start in a configuration where the two plates are distant. It is also possible to activate the shear only when the distance between the two plates is smaller than $6\delta_n$, which is typically when the interaction between the two surfaces can be considered as non negligible according to the XN model. For the simulations, $T_{n_{max}} = 1GPa$ and $\delta_n = 1nm$. The shear interaction has been set to zero in the first place.



2.2 Results

Fig. 3 shows a typical experimental observation of the wavefront bonding observed with an InfraRed camera during the molecular bonding of two silicon wafers (top in Fig. 3). The bright zone corresponds to the bonded region, the darker to the area that is not bonded yet. On the top-left picture, the bonding is initiated on the left of the wafer. Initiation consists of applying a short pressure to trigger the process. Once the bonding propagation is initiated, the wave front runs from left to right. Due to the initiation of the bonding process, the wavefront show initially an almost circular contour but its curvature increases as the bonding extends across the interface.

In the bottom of Fig. 3, we present the results of the finite element simulations. The distribution of the displacement normal to the wafer surfaces is reported. The blue/darker corresponds to the bonded area, and the green-red area (brighter region) to the surface that is not bonded yet. The area where an initial pressure is prescribed to trigger the bonding process is more extended in the simulation compared to the experimental data reported in Fig. 3. Therefore, the curvature of the initial bonding wavefront is larger curvature. During the wavefront propagation, its curvature increases as the bonding extends, toward the middle of the wafer. When the second half of the wafer bonds; the radius of curvature of the bonding wavefront decreases until complete bonding.

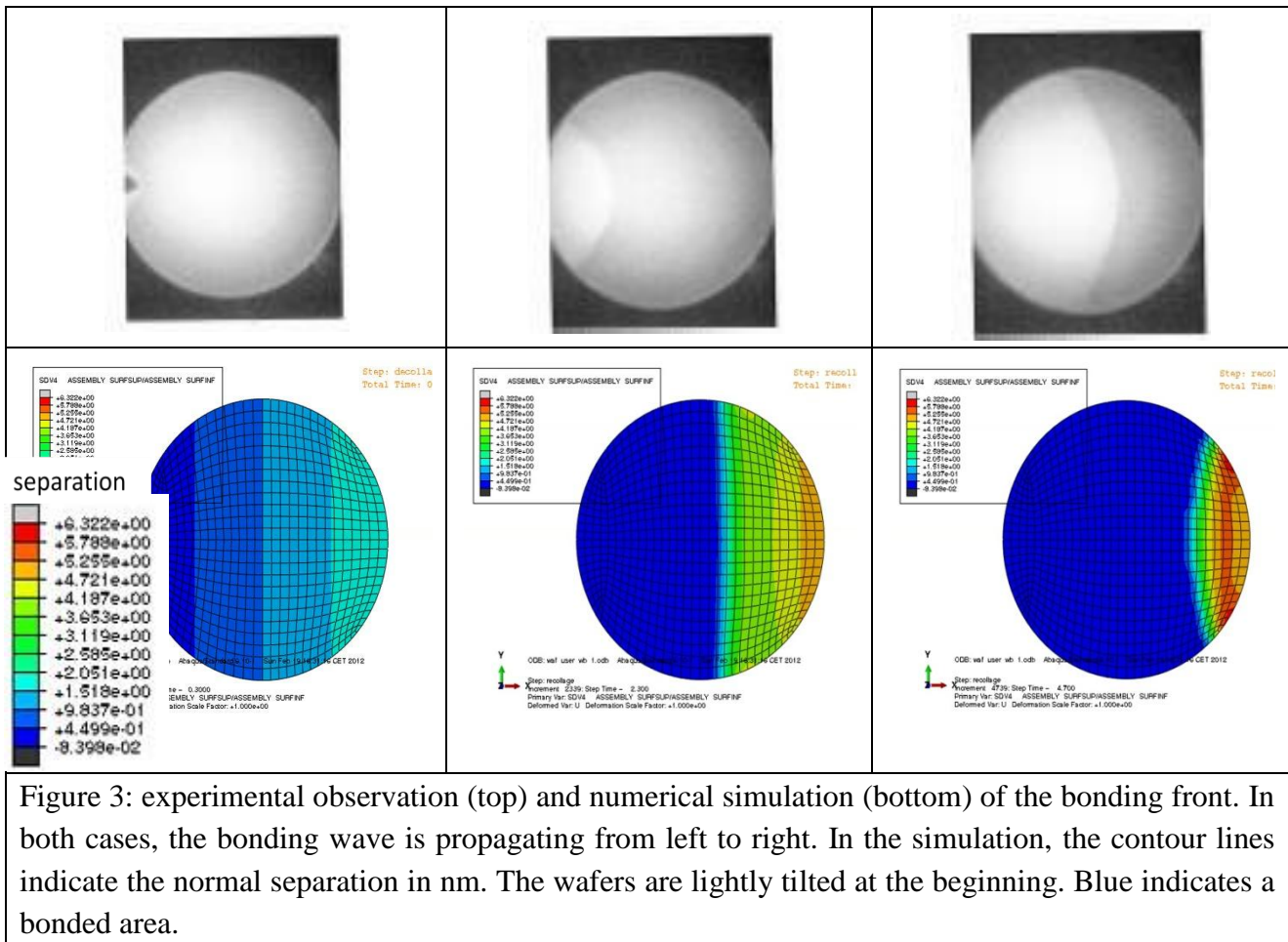


Figure 3: experimental observation (top) and numerical simulation (bottom) of the bonding front. In both cases, the bonding wave is propagating from left to right. In the simulation, the contour lines indicate the normal separation in nm. The wafers are lightly tilted at the beginning. Blue indicates a bonded area.

4. Discussion and Conclusion

We have presented a modeling of the natural bonding between two interactive surfaces by accounting for realistic adhesion interactions, at least qualitatively. The wavefront propagation predicted in our simulations is qualitatively consistent with available data of this problem. The methodology of using a contact mechanics approach to handle the cohesive interaction is found suitable for this problem. We here postulated the cohesive interaction between the two plates but some information can be extracted from the molecular dynamics calculations, in the spirit of a recent work by Kubair et al. [4] for instance. The influence of the cohesive parameters and in particular the magnitude of the maximum traction and that of the adhesion energy are currently under progress. How these could modify the wave front profile and the stress distribution in the plates will be investigated.

References

- [1] A. Prössl and G. Kräuter, Wafer direct bonding: tailoring adhesion between brittle materials, *Materials Science and Engineering*, R25, (1999), 1-88
- [2] F. Rieutord, B. Bataillou and H. Moriceau, Dynamics of a bonding wavefront, *Phys Rev Lett.* 94, (2005),236101
- [3] O. Vallin, K. Jonsson, U. Lindberg, Adhesion quantification methods for wafer bonding, *Materials Science and Engineering*, R50, (2005), 109-165.
- [4] D.V. Kubair, D. J. Cole, L. C. Ciacchi, and S M. Spearing, Multiscale mechanics modeling of direct silicon wafer bonding, *Scripta Materiala*, 60, (2009), 1125-1128
- [5] Abaqus, finite element package, v6.10, Simulia, Dassault Systems
- [6] X.P. Xu and A. Needleman, Numerical simulations fast crack growth in brittle solids, *Journal Mechanics Physics Solids*, 42, (1994), 1397-1434.
- [7] Y.F. Gao and A.F. Bower, A simple technique for avoiding convergence problems in finite element simulations of crack nucleation and growth on cohesive interfaces, *Modell. Simul. Mat. Sci. Engng*, 12, (2004), 453-463